Transmitting Stepwise Rotation among Three Molecule-Gear on the Au(111) Surface

Kwan Ho Au Yeung, Tim Kühne, Frank Eisenhut, Michael Kleinwächter, Yohan Gisbert, Roberto Robles, Nicolas Lorente, Gianaurelio Cuniberti, Christian Joachim, Gwénaël Rapenne, et al.

Transmitting stepwise rotation among three molecule-gears on the Au(111) surface

Kwan Ho Au Yeung[1,2], Tim Kühne[1,2], Frank Eisenhut[1,2], Michael Kleinwächter[3], Yohan Gisbert[3], Roberto Robles[4], Nicolas Lorente[4], Gianaurelio Cuniberti[2], Christian Joachim[3], Gwénaël Rapenne[3,5], Claire Kammerer[3], and Francesca Moresco[1]*

[1]Center for Advancing Electronics Dresden, TU Dresden, 01062 Dresden, Germany

[2]Institute for Materials Science, TU Dresden, 01062 Dresden, Germany

[3]CEMES and Université de Toulouse, CNRS, Toulouse, France

[4]Centro de Física de Materiales CFM/MPC (CSIC-UPV/EHU), 20018 Donostia-San Sebastián, Spain

[5] Division of Materials Science, Nara Institute of Science and Technology, 8916-5 Takayama, Ikoma, Nara, Japan

Corresponding Author

*Correspondence should be addressed to francesca.moresco@tu-dresden.de.

ABSTRACT

The transmission of motion and rotation between molecule-gears have been investigated for two modified designs of star-shaped pentaphenylcyclopentadiene (PPCP) molecules on the Au(111) surface by low-temperature scanning tunneling microscopy. Our experiments show that a tert-butyl group equipping one tooth end of the gear benefits not only the imaging, but also the tip-induced manipulation. An effective anchor allows stable rotations at a fixed point and limits the lateral displacement. On-surface synthesis promotes a radical state of the molecules during molecules deposition or by tip-induced cleaving at the cyclopentadiene core. Our results reveal that such open radical state, also demonstrated by density functional theory calculations, favors the anchoring of the molecule to the surface. Integrating the optimized functions required for molecule-gears, the transmission of rotations up to three interlocked molecule-gears is reported with stepwise and reproducible rotational motions.

KEYWORDS: molecule-gear, molecular machine, STM manipulation, on-surface synthesis, density functional theory

A molecular mechanical machine requires transmission of motions between active components (motors) and passive molecular structures (gears, pull-tabs) to become functional. These devices convert external excitations into rotation, where motors can be triggered by light [1] [2], chemical reactions [3], scanning tunneling microscope (STM) tips [4] [5], or electric field [6]. While the advances in synthetic chemistry and on-surface chemistry allow the rational design of molecule-gears, the rotational mechanics and the corresponding transmission of motion remain a big challenge.

STM offers not only the real-space visualization of a molecule-machine on surfaces, but also local manipulation as an external source of power, for examples, powering nanocars by tunneling current and/or electric field [7] [8], turning on/off molecular switches [9] [10], and inducing chemical reactions [11] [12]. On this account, low-temperature STM in ultra-high vacuum (UHV) is an excellent tool for locally providing external input and monitoring the rotations of the molecular gears under high-stability and clean-imaging conditions.

The first STM experimental study of a single molecule-rotor on a metal surface was performed in 1998, [13] showing lateral translations and continuous rotations of a single hexa-*tert*-butyl decacyclene (HB-DC) molecule were found on the Cu(100) surface at room temperature. Interestingly, the individually rotating molecule could also be controlled by the tip within a void of a monolayer of those molecules. Another breakthrough came several years later, in 2007, when a molecular rack-and-pinion device was demonstrated by using a low-temperature STM, known as the first interlocked molecular gear device [14]. Recently, on a Pb(111) surface, the transmission of motion between two hexa-*tert*-butyl-pyrimidopentaphenylbenzene (HB-NBP) molecules mounted on Cu adatom axes was demonstrated, using a third HB-NBP molecule as a "molecular handle" [15]. Furthermore, as an alternative strategy, one promising result was presented with individual molecule rotating together via dipole-dipole interactions [16]. More examples on the

rotation of molecule-gears with several strategies were presented, like single-molecule rotations on atomic axles [17] [18], and rotations of a gear on top of molecular metallo-organic fragments (*i.e.* deckers or tripods) [19] [20]. Nonetheless, most of these cases are characterized by random (50% clockwise and 50% anticlockwise) directions of rotation, temperature-induced continuous rotation, or by the rotation of only one molecule. The challenges of a highly controlled transmission of rotation within a long train of molecule-gears are not yet resolved.

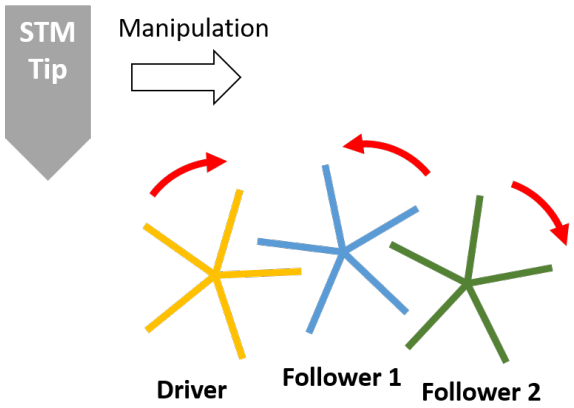

Figure 1. Illustration of a transmission of rotations between 3 star-shaped molecule-gears aligned on a metal surface. The interaction with the STM tip provides the mechanical energy to drive the first gear, namely the Driver gear, so that this gear transmits the rotation to Follower 1 and 2.

Progressing toward a multi-gear assembly and the corresponding transmission of rotation, there are several key factors to be tackled: first, a strong anchoring is necessary for pinning individual molecule-gears at precise interlocking distances and rotating without any lateral displacements. Second, the tip-induced manipulation protocol as an external excitation (tip-molecule interaction) has to be optimized by choosing the appropriate parameters of tip-molecule distance and tunneling current and voltage. Furthermore, a chemical or steric tag is beneficial for a two-dimensional

symmetric molecule to follow its stepwise rotation, where such strategy can provide real-space contrast of the molecular rotation from STM imaging. It is also crucial to consider the optimization for transmitting motion, like the length of the teeth or distance between the molecules. Figure 1 schematically illustrates the outline of the proposed system.

In this paper, we present two chemical modifications within the framework of a star-shaped pentaphenylcyclopentadiene (PPCP) molecule that takes a macroscopic gear as an analogy. As a proof-of-concept, STM lateral manipulations were applied for precisely controlling and analyzing the stepwise rotations and the corresponding quality of anchors. As a first example of a functional multi-gear system, we report on the stable transmission of motion along a train of three molecule-gears.

Pentaphenylcyclopentadiene (PPCP) molecular fragments used in this study incorporate a central planar five-membered ring surrounded by five aromatic groups, thus exhibiting a star-shaped geometry. They are usually obtained from parent precursors bearing an additional C-H or C-halogen bond on the cyclopentadiene core, leading to a radical or anionic state after homolytic or heterolytic bond cleavage, respectively. In this context, anionic PPCP fragments have been intensely used as bulky ligands in organometallic chemistry, and coordination to the metal center can then occur from one, two, three or five carbon atoms located in the ring [21]. In the latter case, the flat and star-shaped PPCP ligand is symmetrically bonded to the metal center, while keeping a privileged rotational degree of freedom around the metal-cyclopentadiene axis. This arrangement has been previously exploited in the design and synthesis of ruthenium-based rotary molecular machines, incorporating an additional tripodal scorpionate ligand as anchoring subunit in view of on-surface studies [19-20, 22].

In the present work, it was envisioned to anchor such star-shaped PPCP fragments directly on a Au(111) surface to construct a molecule-gear, after an homolytic cleavage of the C-Br bond present in the precursor by thermal annealing or application of a local tip-induced voltage pulse. Interaction of the resulting radical state with the substrate would thus provide an axle, ideally favoring rotary motions over translations. In order to monitor the stepwise rotation of PPCP molecular gears by STM, it appeared important to break the five-fold symmetry of the framework and incorporate a marker on one of the teeth. Two strategies have been devised: (1) substitution of a phenyl tooth by a pyrimidine group acting as a chemical tag (gear **1**), and (2) extension of one phenyl tooth with a *tert*-butyl group in *para* position, acting as a steric tag (gear **2**). As reported below, these tags have an important impact on the motions of a single molecule as well as on the intermolecular transmission of motion.

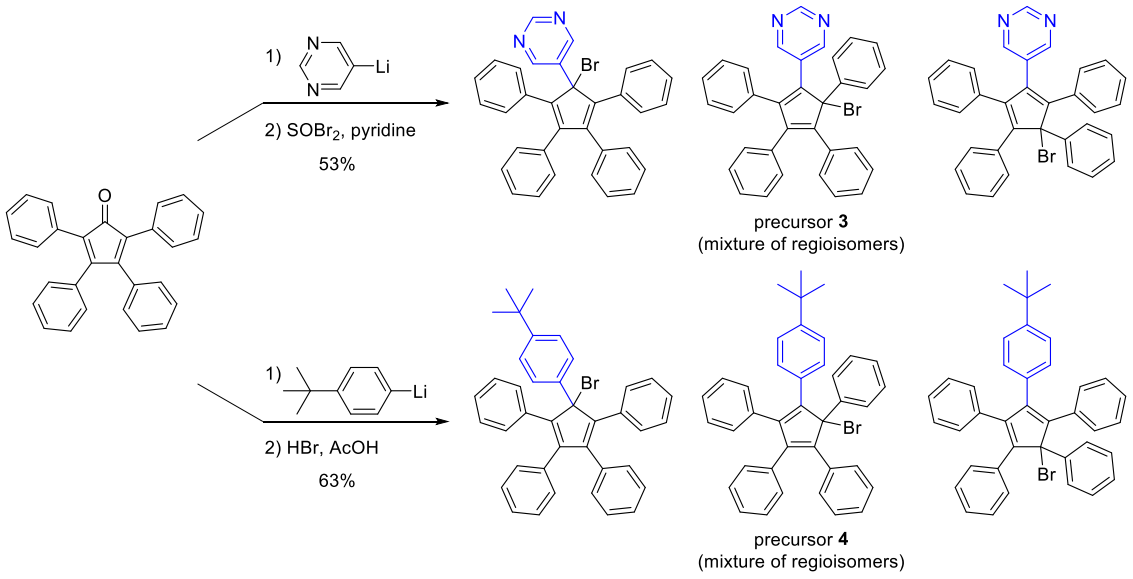

Scheme 1. Structure and synthesis of brominated precursors 3 and 4, incorporating a pyrimidinyl chemical marker and a 4-tert-butylphenyl steric marker, respectively. Precursors 3 and 4 are obtained in two steps from 2,3,4,5-tetraphenylcyclopentadienone as a mixture of three regioisomers.

The brominated precursors of the PPCP-derived molecule-gears **1** and **2** were prepared in two steps from 2,3,4,5-tetraphenylcyclopentadienone by addition of the appropriate aryl lithium species followed by bromination of the intermediate alcohol (Scheme 1). Precursor **3** incorporating a pyrimidinyl group ($C_{33}H_{23}BrN_2$) was obtained with a 53% overall yield as a mixture of three regio-isomers, related to the location of the bromine atom on the different positions of the five-membered ring. According to the same synthetic sequence, precursor **4** displaying a 4-*tert*-butylphenyl moiety ($C_{39}H_{33}Br$) was prepared with a 63% yield, as a mixture of three regioisomers [23]. It is essential to note that, in each case, the three regioisomers of the precursor will give the same molecule as a unique isomer after debromination.

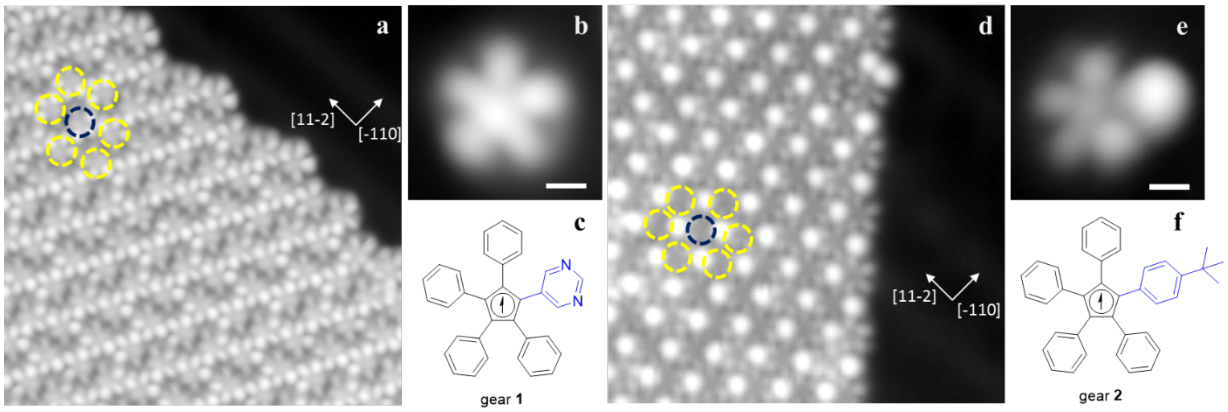

Figure 2. Overviews and the structure of molecule-gears on Au(111). (a – c) The structure of the PPCP-based gear 1 molecule. (a) The STM image (15 nm x 15 nm) was taken under the conditions of V = 500 mV and I = 7.2 pA. (b) STM image of a single gear 1 molecule. Scale bar = 0.5 nm. (c) Chemical structure of a gear 1 molecule. (d - f) The structure of the PPCP-based gear 2 molecule. (d) The STM image (15 nm x 15 nm) was taken under the conditions of V = 500 mV and I = 7.2 pA. Black arrows indicate the orientations of molecules. (e) STM image of a single gear 2 molecule. Scale bar = 0.5 nm. (f) Chemical structure of a gear 2 molecule.

The deposition of precursors **3** and **4** (as mixtures of regioisomers) was achieved by sublimation on the Au(111) at sub-monolayer coverage (see method section for details). As shown in the STM images of Figure 2a and d, closed packed molecular islands were obtained. Smaller islands or groups of a few molecules were also found at the elbows of the herringbone reconstruction of Au(111). Despite the use of precursor samples containing three regioisomers, the pattern of both monolayers appears homogeneous, which can be ascribed to the efficient debromination of the three isomers leading to one single radical species on surface (even though the preferred sublimation of one single isomer cannot be ruled out). For both designs, each gear has six neighbors surrounding, forming a hexagonal structure, as depicted with the dotted circles on Figures 2a and 2d. Note that both dissymmetric structures of gears **1** and **2** reveal slightly uneven patterns compared to the structure of a Au(111) substrate within the island. The nearest-neighbor distance of gear **1** is 1.21 nm +/- 0.01 nm and of gear **2** is 1.36 nm +/- 0.02 nm. The brighter lobes in Figure 2d obtained under STM imaging parameters V = 500 mV and I = 7.2 pA can be easily associated to the *tert*-butyl groups present in gear **2**.

The extraction of single molecules from islands was successful by a gentle STM tip crashing, but not possible by STM lateral manipulation. On Figure 2e, STM image of a single molecule reveals the expected chemical structure of gear **2** depicted on Figure 2f. This confirms that the *tert*-butyl group can act as a steric marker due to its distinguishable apparent height at about 0.22 nm (See Figure S5), relatively higher than the planar phenyl ring at about 0.17 nm on the Au(111) surface. Importantly, such *tert*-butyl group can also be visualized under routine STM imaging condition (V = 500 mV and I = 10 pA), which is a key asset to track stepwise motions.

In the case of gear **1**, the single molecule image (Figure 2b) corresponds to the expected chemical star-shaped structure depicted on Figure 2c, with the five aryl teeth surrounding the central

cyclopentadiene core. Even though lines of maxima are observed in the islands of gear **1** (Figure 2a), such maxima are not visible after separation from the island (Figure 2b). Therefore, it is not clear if these maxima are related to the pyrimidine groups. Pyrimidine moieties have already been successfully used as chemical markers in previous studies involving HB-NBP molecules, inducing contrast at bias voltage above 2.2 V on a Cu(111) surface [14]. Nevertheless, in our case on Au(111), we observed none of the mentioned features also varying the bias voltage, indicating that under such conditions the pyrimidine group cannot be exploited as a chemical tag. The same absence of electronic tag effects was observed for the HB-NBP molecule on Pb(111) [15] suggesting that on Au(111) and Pb(111), the pyrimidine moiety adopt a surface conformation reducing its electronic interactions with the surface.

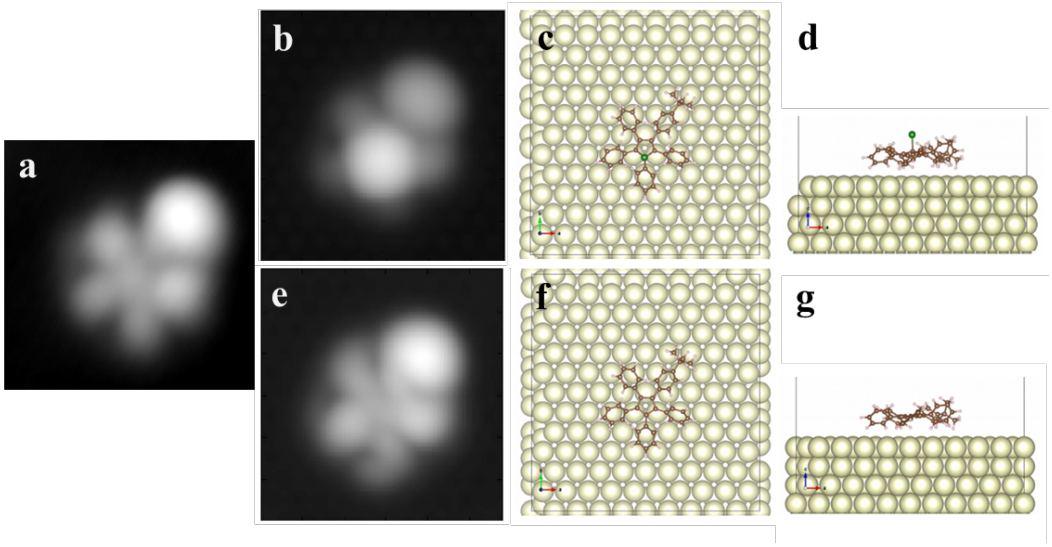

Figure 3. DFT simulations of precursor 4 and radical state of molecule-gear 2 on Au(111). (a, b, e) Comparison of the experimental and simulated STM images. (a) Experimental image of a gear **2** molecule. The image (2.75 nm x 2.75 nm) was taken under V = 500 mV and I = 7.2 pA. (b) A simulated constant-current image of gear **2** molecule with a C-Br bond at the cyclopentadiene core. (e) A simulated image of precursor **4** (one regioisomer) displaying after cleaving the C-Br

bond at the core. The voltage bias of the simulations was V = 1.0 V. (c – d, f – g) Top and side views of the simulated adsorption geometries from gear **2** molecules with (e) a precursor **4** and (e) gear **2** molecule.

Beside the presence of a tag to monitor a motion, another decisive property is to anchor individual molecule- gears on the surface so that their teeth can engage at a particular distance and the degrees of freedom along the gear train can be limited. A robust anchoring allows a stable rotational motion and limits the lateral displacement during manipulation. By analogy with the coordination of PPCP rotary platforms to ruthenium centers in organometallic molecular machines [19 24], it was envisioned to anchor the PPCP gears on the Au(111) substrate via carbon-metal bonds. To this aim, precursors **3** and **4** incorporate a bromine atom on the central ring, since this halogen affords a good balance between precursors stability and ease of homolytic C-halogen bond cleavage. Practically, by voltage pulsing with the tip (we generally apply from + 2.0 to + 3.0 V under 10 s) at the cyclopentadiene core or during on-surface annealing, the bromide group is cleaved, dehalogenation of the precursors occurs, leading to gears structures **1** and **2**. As a result, the radical state of the de-halogenated molecules leads to a new metal-organic bond with the Au(111) substrate (Figure S6) that can serve as an axle for rotation. To gain further insight in such molecule-substrate interactions, DFT calculations were performed. From Figure 3e, the DFT simulated STM image of gear **2** has a good agreement with the experimental image (Figure 3a), where it confirms the conformation of **2** and successful debromination on surface. Indeed, in the simulated STM image of precursor **4** (Figure 3b), the presence of the bromine atom pointing away from the surface (Figure 3d) is easily identified. Furthermore, DFT calculations (Figure 3f, g) reveal the adsorption geometry of gear **2** molecules on Au(111), with the central cyclopentadiene plane parallel to the surface. This highlights the likely contribution of the five carbon atoms of the

ring to the bonding with the metal atoms underneath, as expected from the delocalized nature of the cyclopentadienyl radical.

The anchoring strategy was subsequently tested in lateral manipulation experiments to probe the possibility for gears **1** and **2** to undergo concentric motions. Surprisingly, with the same anchoring strategy, gear **1** fails to show concentric rotational motions (Figure 4) while most of the gear **2** molecules reproducibly rotate (Figure 5). As discussed in the following, this observation further confirms that, more than a simple marker, such a *tert*-butyl group also plays an important role on stabilizing the molecular gears on metal surfaces [25] [26], and facilitating the rotation.

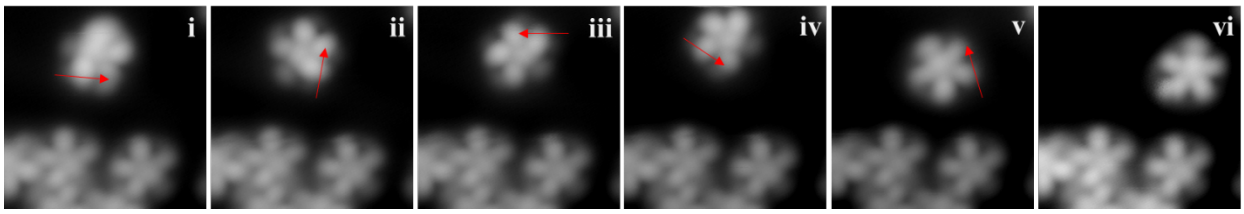

Figure 4. Non-concentric rotation of a single molecule-gear 1. Red arrows indicated the trajectories of lateral manipulations (V = 10 mV, I = 8 pA; Tunneling resistance = 1.25 GΩ) achieved by the STM tip. (i – ii) Only the first step of manipulation generated a concentric rotation. (iii – vi) The rest of manipulations induced both rotations and small lateral shifts. All STM images (5 nm x 5 nm) were taken under the conditions of V = 500 mV and I = 7.2 pA.

Figure 4 shows a stepwise rotation sequence of gear **1** imaged by the STM. All lateral manipulations (red arrows) were applied in constant current mode. The STM captures images before and after each manipulation in all the following sequences. All the steps show successful movements induced by the STM tip, however, only step 1 (i – ii) shows a concentric rotation while the rest shows small lateral shifts with some degrees of rotations. During both imaging and lateral manipulation, the molecules could be easily picked up by the STM tip at very low tunneling current

(I = 8 - 10 pA). A total of five lateral manipulations were performed (see red arrows) where the tip apex travelled across one of the teeth towards the next teeth in constant current mode. Transmitting rotations between gear **1** molecules have been attempted, however, only movements like the ones reported in ref. [15] for a single HB-NBP molecule-gear have been observed, as shown in Figure S7.

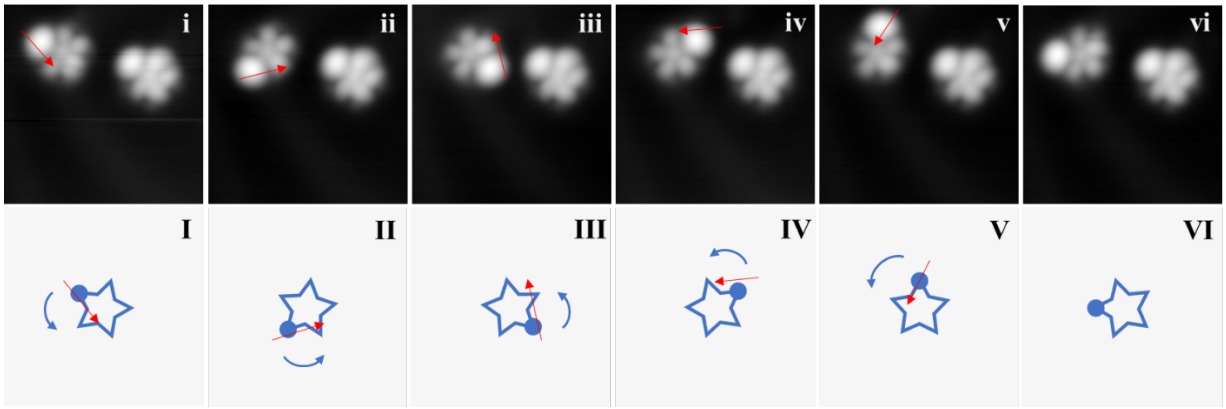

Figure 5. Rotation of a single molecule-gear 2. Red arrows indicate the trajectories of lateral manipulations (V = 10 mV and I = 8 pA; Tunneling resistance = 1.25 GΩ) achieved by the STM tip. (i - vi) Rotational sequence of a single molecular gear **2**. The molecule on the right acts as a reference. (I – VI) Corresponding schematic diagrams of the gear rotations (not in scale). All STM images (6.5 nm x 6.5 nm) were taken under the conditions of V = 530 mV and I = 13 pA. (Movie S1)

Figure 5 shows a step-by-step and complete rotation of a single molecule gear **2** in an anti-clockwise direction by five manipulations. All lateral manipulations (red arrows) were applied in constant-current mode. The rotational angles are in average 84° and we observed a maximum total rotation of 419°. Note that the rotations of the single gear are concentric, indicating that the interaction between the cyclopentadienyl radical and the surface successfully and strongly anchors the gear at the pinning position determined by DFT calculations (See Figure 3).

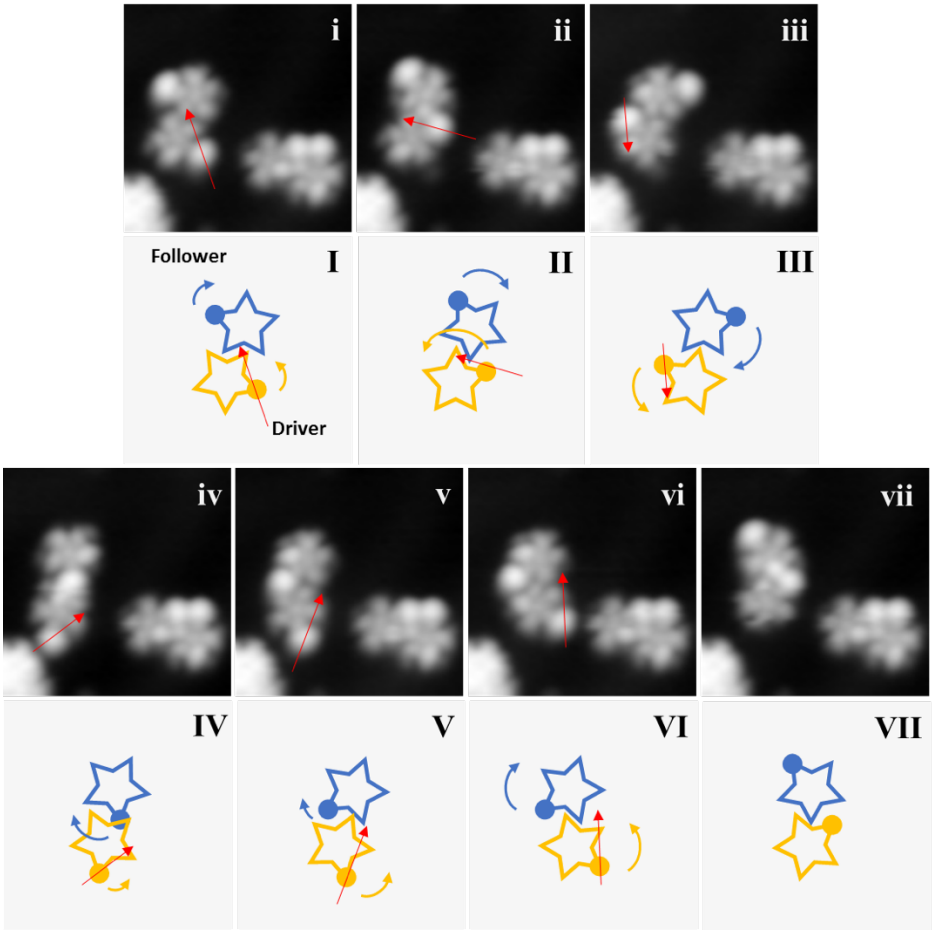

Figure 6. Stepwise collective rotational sequence between two single molecule-gears 2. Red arrows indicate the trajectories of lateral manipulations (V = 10 mV and I = 14 pA; Tunneling resistance = 0.71 GΩ) achieved by the STM tip. (i – vii) The rotations between two gear **2** molecules. The other two molecules on the right act as a reference and their motion sequence is shown in Figure S7. (I – VII) Corresponding schematic diagrams of the gear rotations (not in scale). All STM images (6.5 nm x 6.5 nm) were taken under the conditions of V = 530 mV and I = 13 pA. (Movie S2)

Isolation of individual gear **2** molecules (Figures 5 – 7) was achieved by gently crashing the STM tip near a molecular island (Figure 2d). Smaller groups of 2 – 4 molecule trains formed after

the tip crashing, therefore, it was possible to obtain a sufficient amount of coupled gears. From Figure 6, a sequence of stepwise and complete rotations of two meshing molecular gears is demonstrated. A sequence of six lateral manipulations are performed (See trajectories indicated by red arrows). The gear-to-gear distance in this case is 1.35 nm. The STM tip drives the driver gear by interacting with the *tert*-butyl tooth in order to generate an anti-clockwise rotation. Simultaneously, such anti-clockwise rotation mechanically transmits to the follower gear. As a result, the follower gear rotates clockwise. From the whole sequence (Figure 6), each rotational angle is on average 83° for the driver and 68° for the follower; totally 499° for the driver and 410° for the follower. Interestingly, larger rotational angles between steps 2 – 3 (Figure 6ii – iii; angle: 122°) and 3 – 4 (Figure 6iii – iv; angle: 116°) are observed while the *tert*-butyl teeth of the gear directly interact with the phenyl rings of the other. This is possibly due to a larger repulsive interaction between the *tert*-butyl groups and phenyl rings. Furthermore, a small lateral displacement (about 0.4 nm) of the driver gear is observed between steps 5 – 6 (Figure 6v – vi). One additional step (Figure 6vi – vii) was needed to achieve a full rotation on the follower due to the insufficient motion between steps 5 – 6 (Figure 6v – vi; angle: 4°). It is worth to notice that as previous simulations [27] [28] [29] suggest, due to the expected "soft gear" effect, the follower is experiencing smaller rotational angles than the driver. Many degrees of freedom of the follower are activated while pushing on the driver as observed in [15]. In other words, the collective rotational degrees of freedom of the follower, activated by the STM tip, are in competition with many other possible intramolecular mechanical modes.

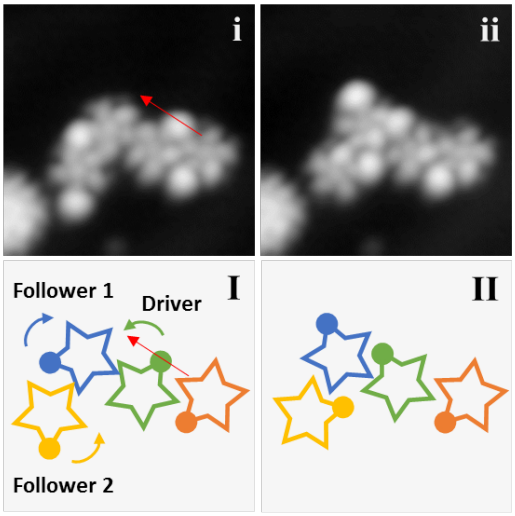

Figure 7. Stepwise collective rotational sequence between three single molecule-gears 2. Red arrows indicate the trajectories of lateral manipulation (V = 10 mV and I = 14 pA; Tunneling resistance = 0.71 GΩ) achieved by the STM tip. (i – ii) STM tip manipulation at the third gear as a driver induced a three-in-a-train collective rotation. The gear on the right side did not mesh with the driver, hence, no rotation was observed. (I – II) Corresponding schematic diagrams of the gear rotations (not in scale). All STM images (6.5 nm x 6.5 nm) were taken under the conditions of V = 530 mV and I = 1.9 pA.

Transmitting a rotation along a train of gears is an essential prerequisite for the construction of mechanical molecular machines. To the best of our knowledge, there was no transmission of rotations realized between more than two molecule-gears [15]. Here, we present a collective transmission of rotation between three molecule-gears **2** (Figure 7). While manipulating (red arrow) the *tert*-butyl tooth of the third gear as a driver (Figure 7i) by the STM tip, we induced a step of transmission of rotation between three meshing gears. The scene is described as follows: an anticlockwise rotation from the driver (green) initiates a clockwise rotation for 64° the follower 1 (blue), then simultaneously results to an anticlockwise rotation for 78° at the follower 2 for 104°

(orange) (Figure 7i – ii). The gear-to-gear distance between driver and follower 1 is 1.19 nm, and 1.37 nm between the two followers. Note that the gear on the right side (brown) did not mesh with the driver at a sufficient distance, hence, no rotation was observed. Nevertheless, no further rotation after this scenario was observed within the same train of molecules possibly due to the interlocking of *tert*-butyl groups between gears.

Comparison of the motions of the two proposed designs reveals that only gear **2** showed transmission of rotation up to three meshing gears. Given that the tunneling resistances are very similar (0.71 – 1.25 GΩ) during the manipulations of both gears in the constant-current mode, the driving potential energy increase are nearly the same in all rotations. In addition, assuming that the interactions between the bare phenyl rings from both gears **1** and **2** are the same, we suggest that during STM manipulation, the presence of the *tert*-butyl group of gear **2** provides a more favorable tip-gear interaction than the planar phenyl ring of gear **1**.

The increase of potential energy induced by the tip manipulating the *tert*-butyl group of the driver allows the train of three gears to find a minimum energy path on the corresponding ground state potential energy surface (PES), and thus makes the transmission of rotation along the train possible. The end of the scenario indicates that after following this minimal energy path, a deep minimum energy well is existing on the PES of those three molecules interacting together which is stabilizing the final conformation imaged in Figure 7 ii.

For assemblies of more than three molecule-gears in a train, we have not observed any successful transmission of rotation. A possible reason is that the tip-induced potential energy increase of the driver is not able in this case to excite the rotational degrees of freedom of the followers but is directed towards others degrees of freedom on the PES.

We have presented a sequence of rotation transmission along a train of gears up to three meshed molecule-gears. Our observations shed light on the challenges concerning the quality of the anchoring strategy, of the visualization by a chemical or a steric tag and of tip-induced manipulations. The design rules are interdependent because a very specific minimal energy path is expected on the ground state potential energy surface of the train to observe a transmission of rotation. For example, a steric *tert*-butyl tag can benefit from the tip-induced manipulations and stabilize the gear but simultaneously hinder the transmission of rotation because a large potential energy increase will deviate from the expected minimal energy path. As a next challenge, the controllability of rotating a larger number of gears in a train is especially critical for the development of molecular mechanical machines, like mechanical calculators.

Both modified PPCP precursor **3** and **4** molecules were evaporated at 458 K and 441 K respectively for 30 s on a Au(111) surface kept at room temperature. The samples were cleaned by subsequent cycles of Ar sputtering and annealing to 723 K. STM experiments were performed using a custom-built instrument operating at a low temperature of T = 5 K and ultrahigh vacuum ($p \approx 1 \times 10^{-10}$ mbar) conditions. All shown STM images were recorded in constant-current mode with the bias voltage applied to the sample.

DFT calculations have been performed using the VASP code [30]. Core electrons have been treated using the projector augmented-wave method [31] [32]and wave functions have been expanded using a plane-wave basis set with an energy cutoff of 400 eV. Exchange and correlation energies have been treated within the generalized gradient approximation in the PBE form [33]. Missing van der Waals interactions have been added using the Tkatchenko-Scheffler scheme [34]. The Au(111) surface has been modeled using a slab geometry with four layers in a 10x6√3 surface supercell and a vacuum region of ~19 Å. Top two Au layers and the molecule have been relaxed until all

the forces where smaller than 0.02 eV/Å. STM topographic images have been simulated within the Tersoff-Hamann approximation [35] [36] using the method by Bocquet *et al* [32] as implemented in STMpw [33].

ASSOCIATED CONTENT

Supporting Information.

The following file containing details on the chemical synthesis, additional experimental data, and additional theoretical results is available free of charge (PDF).

Author Contributions

All authors discussed the results and contributed to the manuscript. The manuscript was written through contributions of all authors. All authors have given approval to the final version of the manuscript.

ACKNOWLEDGMENT

This work was supported by the European Union Horizon 2020 FET open project "Mechanics with Molecule(s)" (MEMO, Grant 766864), the University Paul Sabatier (Toulouse, France) and CNRS. This research was also partly supported by the JSPS KAKENHI grant in aid for Scientific Research on Innovative Areas "Molecular Engine (No.8006)" 18H05419. Y.G. thanks the MESR for a PhD Fellowship.

REFERENCES

1. Kassem, S.; van Leeuwen, T.; Lubbe, A. S.; Wilson, M. R.; Feringa, B. L.; Leigh, D. A., Artificial molecular motors. *Chemical Society Reviews* **2017,** *46* (9), 2592-2621.
2. Koumura, N.; Zijlstra, R. W. J.; van Delden, R. A.; Harada, N.; Feringa, B. L., Light-driven monodirectional molecular rotor. *Nature* **1999,** *401* (6749), 152-155.
3. Vale, R. D.; Milligan, R. A., The Way Things Move: Looking Under the Hood of Molecular Motor Proteins. *Science* **2000,** *288* (5463), 88.
4. Henningsen, N.; Franke, K. J.; Torrente, I. F.; Schulze, G.; Priewisch, B.; Rück-Braun, K.; Dokić, J.; Klamroth, T.; Saalfrank, P.; Pascual, J. I., Inducing the Rotation of a Single Phenyl Ring with Tunneling Electrons. *The Journal of Physical Chemistry C* **2007,** *111* (40), 14843-14848.
5. Soe, W.-H.; Shirai, Y.; Durand, C.; Yonamine, Y.; Minami, K.; Bouju, X.; Kolmer, M.; Ariga, K.; Joachim, C.; Nakanishi, W., Conformation Manipulation and Motion of a Double Paddle Molecule on an Au(111) Surface. *ACS Nano* **2017,** *11* (10), 10357-10365.
6. Seldenthuis, J. S.; Prins, F.; Thijssen, J. M.; van der Zant, H. S. J., An All-Electric Single-Molecule Motor. *ACS Nano* **2010,** *4* (11), 6681-6686.
7. Kudernac, T.; Ruangsupapichat, N.; Parschau, M.; Maciá, B.; Katsonis, N.; Harutyunyan, S. R.; Ernst, K.-H.; Feringa, B. L., Electrically driven directional motion of a four-wheeled molecule on a metal surface. *Nature* **2011,** *479* (7372), 208-211.
8. Pawlak, R.; Meier, T.; Renaud, N.; Kisiel, M.; Hinaut, A.; Glatzel, T.; Sordes, D.; Durand, C.; Soe, W.-H.; Baratoff, A.; Joachim, C.; Housecroft, C.; Constable, E.; Meyer, E., Design and Characterization of an Electrically Powered Single Molecule on Gold. *ACS Nano* **2017,** *11*.
9. Liljeroth, P.; Repp, J.; Meyer, G., Current-Induced Hydrogen Tautomerization and Conductance Switching of Naphthalocyanine Molecules. *Science* **2007,** *317* (5842), 1203.
10. Auwärter, W.; Seufert, K.; Bischoff, F.; Ecija, D.; Vijayaraghavan, S.; Joshi, S.; Klappenberger, F.; Samudrala, N.; Barth, J. V., A surface-anchored molecular four-level conductance switch based on single proton transfer. *Nature Nanotechnology* **2012,** *7* (1), 41-46.
11. Zhao, A.; Li, Q.; Chen, L.; Xiang, H.; Wang, W.; Pan, S.; Wang, B.; Xiao, X.; Yang, J.; Hou, J. G.; Zhu, Q., Controlling the Kondo Effect of an Adsorbed Magnetic Ion Through Its Chemical Bonding. *Science* **2005,** *309* (5740), 1542.
12. Lauhon, L. J.; Ho, W., Single-Molecule Chemistry and Vibrational Spectroscopy: Pyridine and Benzene on Cu(001). *The Journal of Physical Chemistry A* **2000,** *104* (11), 2463-2467.
13. Gimzewski, J.; Joachim, C.; Schlittler, R. R.; Langlais, V.; Tang, H.; Johannsen, I., Rotation of a Single Molecule Within a Supramolecular Bearing. *Science* **1998,** *281*, 531-3.
14. Chiaravalloti, F.; Gross, L.; Rieder, K.-H.; Stojkovic, S. M.; Gourdon, A.; Joachim, C.; Moresco, F., A rack-and-pinion device at the molecular scale. *Nature Materials* **2007,** *6* (1), 30-33.
15. Soe, W.-H.; Srivastava, S.; Joachim, C., Train of Single Molecule-Gears. *The Journal of Physical Chemistry Letters* **2019,** *10* (21), 6462-6467.
16. Simpson, G. J.; García-López, V.; Daniel Boese, A.; Tour, J. M.; Grill, L., How to control single-molecule rotation. *Nature Communications* **2019,** *10* (1), 4631.
17. Manzano, C.; Soe, W. H.; Wong, H. S.; Ample, F.; Gourdon, A.; Chandrasekhar, N.; Joachim, C., Step-by-step rotation of a molecule-gear mounted on an atomic-scale axis. *Nature Materials* **2009,** *8* (7), 576-579.

18. Gao, L.; Liu, Q.; Zhang, Y. Y.; Jiang, N.; Zhang, H. G.; Cheng, Z. H.; Qiu, W. F.; Du, S. X.; Liu, Y. Q.; Hofer, W. A.; Gao, H. J., Constructing an Array of Anchored Single-Molecule Rotors on Gold Surfaces. *Physical Review Letters* **2008,** *101* (19), 197209.
19. Perera, U. G. E.; Ample, F.; Kersell, H.; Zhang, Y.; Vives, G.; Echeverria, J.; Grisolia, M.; Rapenne, G.; Joachim, C.; Hla, S. W., Controlled clockwise and anticlockwise rotational switching of a molecular motor. *Nature Nanotechnology* **2013,** *8* (1), 46-51.
20. Zhang, Y.; Kersell, H.; Stefak, R.; Echeverria, J.; Iancu, V.; Perera, U. G. E.; Li, Y.; Deshpande, A.; Braun, K. F.; Joachim, C.; Rapenne, G.; Hla, S. W., Simultaneous and coordinated rotational switching of all molecular rotors in a network. *Nature Nanotechnology* **2016,** *11* (8), 706-712.
21. Field, L. D.; Lindall, C. M.; Masters, A. F.; Clentsmith, G. K. B., Penta-arylcyclopentadienyl complexes. *Coordination Chemistry Reviews* **2011,** *255* (15), 1733-1790.
22. Kammerer, C.; Rapenne, G., Scorpionate Hydrotris(indazolyl)borate Ligands as Tripodal Platforms for Surface-Mounted Molecular Gears and Motors. *European Journal of Inorganic Chemistry* **2016,** *2016* (15-16), 2214-2226.
23. Vives, G.; Rapenne, G., Directed synthesis of symmetric and dissymmetric molecular motors built around a ruthenium cyclopentadienyl tris(indazolyl)borate complex. *Tetrahedron* **2008,** *64* (50), 11462-11468.
24. Erbland, G.; Abid, S.; Gisbert, Y.; Saffon-Merceron, N.; Hashimoto, Y.; Andreoni, L.; Guérin, T.; Kammerer, C.; Rapenne, G., Star-Shaped Ruthenium Complexes as Prototypes of Molecular Gears. *Chemistry – A European Journal* **2019,** *25* (71), 16328-16339.
25. Otero, R.; Hümmelink, F.; Sato, F.; Legoas, S. B.; Thostrup, P.; Lægsgaard, E.; Stensgaard, I.; Galvão, D. S.; Besenbacher, F., Lock-and-key effect in the surface diffusion of large organic molecules probed by STM. *Nature Materials* **2004,** *3* (11), 779-782.
26. Schunack, M.; Linderoth, T. R.; Rosei, F.; Lægsgaard, E.; Stensgaard, I.; Besenbacher, F., Long Jumps in the Surface Diffusion of Large Molecules. *Physical Review Letters* **2002,** *88* (15), 156102.
27. Zhao, R.; Qi, F.; Zhao, Y.-L.; Hermann, K. E.; Zhang, R.-Q.; Van Hove, M. A., Interlocking Molecular Gear Chains Built on Surfaces. *The Journal of Physical Chemistry Letters* **2018,** *9* (10), 2611-2619.
28. MacKinnon, A., Quantum gears: a simple mechanical system in the quantum regime. *Nanotechnology* **2002,** *13* (5), 678-681.
29. Lin, H. H.; Croy, A.; Gutierrez, R.; Joachim, C.; Cuniberti, G., Mechanical Transmission of Rotational Motion between Molecular-Scale Gears. *Physical Review Applied* **2020,** *13* (3), 034024.
30. Kresse, G.; Furthmüller, J., Efficiency of ab-initio total energy calculations for metals and semiconductors using a plane-wave basis set. *Computational Materials Science* **1996,** *6* (1), 15-50.
31. Blöchl, P. E., Projector augmented-wave method. *Physical Review B* **1994,** *50* (24), 17953-17979.
32. Kresse, G.; Joubert, D., From ultrasoft pseudopotentials to the projector augmented-wave method. *Physical Review B* **1999,** *59* (3), 1758-1775.
33. Perdew, J. P.; Burke, K.; Ernzerhof, M., Generalized Gradient Approximation Made Simple. *Physical Review Letters* **1996,** *77* (18), 3865-3868.

34. Tkatchenko, A.; Scheffler, M., Accurate Molecular Van Der Waals Interactions from Ground-State Electron Density and Free-Atom Reference Data. *Physical Review Letters* **2009,** *102* (7), 073005.
35. Tersoff, J.; Hamann, D. R., Theory and Application for the Scanning Tunneling Microscope. *Physical Review Letters* **1983,** *50* (25), 1998-2001.
36. Tersoff, J.; Hamann, D. R., Theory of the scanning tunneling microscope. *Physical Review B* **1985,** *31* (2), 805-813.

Supporting Information

Transmitting stepwise rotation between three molecular gears on the Au(111) surface by STM

Kwan Ho Au Yeung[1,2], Tim Kühne[1,2], Frank Eisenhut[1,2], Gianaurelio Cuniberti[2], Michael Kleinwächter[3], Yohan Gisbert[3], Roberto Robles[4], Nicolas Lorente[4], Gwénaël Rapenne[3,5], Christian Joachim[3], and Francesca Moresco[1]*

[1] Center for Advancing Electronics Dresden, TU Dresden, 01062 Dresden, Germany

[2] Institute for Materials Science, TU Dresden, 01062 Dresden, Germany

[3] CEMES, Université de Toulouse, CNRS, Toulouse, France

[4] Centro de Física de Materiales CFM/MPC (CSIC-UPV/EHU), 20018 Donostia-San Sebastián, Spain

[5] Division of Materials Science, Nara Institute of Science and Technology, 8916-5 Takayama, Ikoma, Nara, Japan

Table of Contents

1 Chemical synthesis of the precursors

I. Materials and methods

Compound **4** was synthesized according to the published procedure [1], and the characterization data matched those reported in literature [2].
All commercially available chemicals were of reagent grade and were used without further purification unless otherwise stated. Anhydrous THF, anhydrous diethyl ether, *n*-butyllithium (2.5 M in hexanes), thionyl bromide and pyridine were purchased from Aldrich. 5-Bromopyrimidine was purchased from Acros and 2,3,4,5-tetraphenylcyclopenta-2,4-dienone from TCI. All reactions were carried out using standard Schlenk techniques under an argon atmosphere. Column chromatography was carried out on 230–400 mesh silica gel (Aldrich). Thin layer chromatography (TLC) was performed on pre-coated aluminum-backed silica gel 60 UV_{254} plates (Macherey–Nagel) with visualization effected using ultraviolet irradiation (λ = 254, 366 nm).
NMR, mass spectra and elemental analysis were recorded by the appropriate services of the Toulouse Institute of Chemistry (ICT – FR2599). ^{1}H and ^{13}C NMR spectra were recorded on a Bruker Avance 300 MHz (5 mm BBO BB-1H Z-GRD probe) spectrometer. Residual solvent signals were used as internal reference for ^{1}H and ^{13}C NMR. Chemical shifts (δ) are reported in ppm and the following abbreviations have been used to describe the signals: singlet (s); multiplet (m). High-resolution mass spectra (HRMS) were performed with a Waters Xevo G2 QTof spectrometer for electrospray ionization (ESI). Elemental analysis was performed using a PerkinElmer 2400 CHNS/O Series II System.

II. Synthesis of 5-bromo-1,2,3,4-tetraphenyl-5-(pyrimidin-5'-yl)cyclopenta-1,3-diene (3) (Obtained as a mixture of 3 regioisomers)

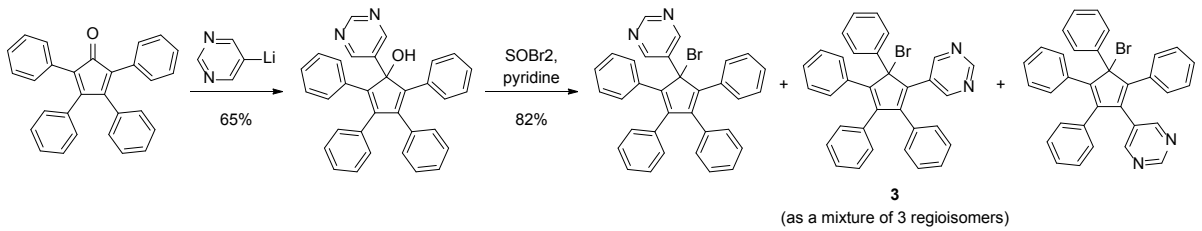

Scheme S1: Synthesis of PPCP-based gear **1**

5-Bromopyrimidine (620 mg, 3.9 mmol, 1.5 eq.) was placed in a Schlenk flask with a stir bar, and anhydrous THF (10 mL) was added. The solution was quickly degassed by bubbling argon and cooled down to -78 °C. Then, a 2.5M solution of *n*-buthyllithium in hexanes (2 mL, 5.2 mmol, 2 eq.) was added dropwise while carefully maintaining the temperature. The suspension was stirred for 30 minutes at this temperature and a degassed solution of 2,3,4,5-tetraphenylcyclopenta-2,4-dienone (1000 mg, 2.6 mmol, 1 eq.) in 30 mL of anhydrous THF was added dropwise via a cannula. The reaction was stirred for two hours at -78 °C before being neutralized by pouring it slowly to 20 mL of a saturated ammonium chloride solution. The crude product was then extracted with diethyl ether, washed three times with water and once with brine. The organic layer was dried over magnesium sulfate and the solvents were removed under vacuum. The crude product was adsorbed onto SiO_2 and purified by a quick column chromatography on SiO_2, eluting impurities with

dichloromethane followed by pure ethyl acetate to collect the product. Solvents were evaporated to afford a yellow solid, still contaminated with impurities. This solid was then recrystallized from a minimal amount of boiling chloroform, to give pure 2,3,4,5-tetraphenyl-1-(pyrimidin-5'-yl)cyclopenta-2,4-dien-1-ol as a clear white solid in a 65% yield (780 mg, 1.7 mmol).

2,3,4,5-Tetraphenyl-1-(pyrimidin-5'-yl)cyclopenta-2,4-dien-1-ol (200 mg, 0.43 mmol, 1 eq.) was subsequently placed in a Schlenk tube containing a magnetic stir bar and anhydrous diethyl ether (10 mL) and freshly distilled pyridine (44 µL, 0.54 mmol, 1.25 eq.) were added. The mixture was cooled down to -10 °C and thionyl bromide (42 µL, 0.54 mmol, 1.25 eq.) was added. The medium was then allowed to warm up to room temperature over one hour, under stirring. It was then neutralized by adding it slowly to 20 mL of a 1M HCl aqueous solution. The product was extracted with ethyl acetate (150 mL), and washed three times with water (3x150 mL). The organic layer was dried over magnesium sulfate and the solvents were removed by rotary evaporation. The crude product was purified by column chromatography (SiO_2, EtOAc/cyclohexane 1:9) to afford the desired brominated product. Nevertheless, traces of impurities were still observed in some batches, so the product was further recrystallized from boiling heptane and rinsed with ice-cold pentane to give pure compound **3** in 82% yield (187 mg, 0.36 mmol, 53% yield over two steps), as a yellow solid composed of a 66:30:4 mixture of regioisomers.

R_f = 0.41 (SiO_2, EtOAc/hexane 3:7);

^{1}H NMR (300 MHz, CD_2Cl_2, 25 °C, mixture of regioisomers): δ = 9.05 (s, 0.04H, Ha_{regio3}), 8.91 (s, 0.30H, Ha_{regio2}), 8.86 (s, 0.66H, Ha_{regio1}), 8.78 (s, 0.08H, Hb_{regio3}), 8.27 (s, 1.32H, Hb_{regio1}), 8.24 (s, 0.60H, Hb_{regio2}), 7.55-7.46 (m, 2H, H_{Ph}), 6.84-7.36 (m, 18H, H_{Ph}) ppm;

^{13}C{^{1}H} NMR (75 MHz, CD_2Cl_2, 25 °C, mixture of regioisomers): δ = 157.6 (C_{pyr}-H), 157.6 (C_{pyr}-H), 157.3 (C_{pyr}-H), 157.2 (C_{pyr}-H), 156.4 (C_{pyr}-H), 150.2 (C_{quat}), 145.5 (C_{quat}), 142.4 (C_{quat}), 142.2 (C_{quat}), 134.9 (C_{quat}), 134.8 (C_{quat}), 134.5 (C_{quat}), 134.4 (C_{quat}), 134.0 (C_{quat}), 133.9 (C_{quat}), 133.5 (C_{quat}), 131.1 (C_{Ph}-H), 130.9 (C_{Ph}-H), 130.7 (C_{Ph}-H), 130.6 (C_{Ph}-H), 130.3 (C_{Ph}-H), 130.3 (C_{Ph}-H), 130.1 (C_{Ph}-H), 129.3 (C_{Ph}-H), 129.3 (C_{Ph}-H), 129.0 (C_{Ph}-H), 128.9 (C_{Ph}-H), 128.7 (C_{Ph}-H), 128.7 (C_{Ph}-H), 128.5 (C_{Ph}-H), 128.4 (C_{Ph}-H), 128.4 (C_{Ph}-H), 128.3 (C_{Ph}-H), 128.3 (C_{Ph}-H), 128.3 (C_{Ph}-H), 128.1 (C_{Ph}-H), 128.0 (C_{Ph}-H), 128.0 (C_{Ph}-H), 128.0 (C_{Ph}-H), 127.9 (C_{Ph}-H), 127.7 (C_{Ph}-H), 75.9 (C_{quat}-Br) ppm;

HRMS (ESI$^+$): calcd. for $C_{33}H_{24}BrN_2$ $[MH]^+$: 529.1108, found 529.1114.

Elemental analysis (%) calcd. for $C_{33}H_{23}BrN_2$: C 75.14, H 4.40, N 5.31; found: C 75.0, H 4.18, N 5.26.

III. ^{1}H and ^{13}C NMR spectra of compound 3

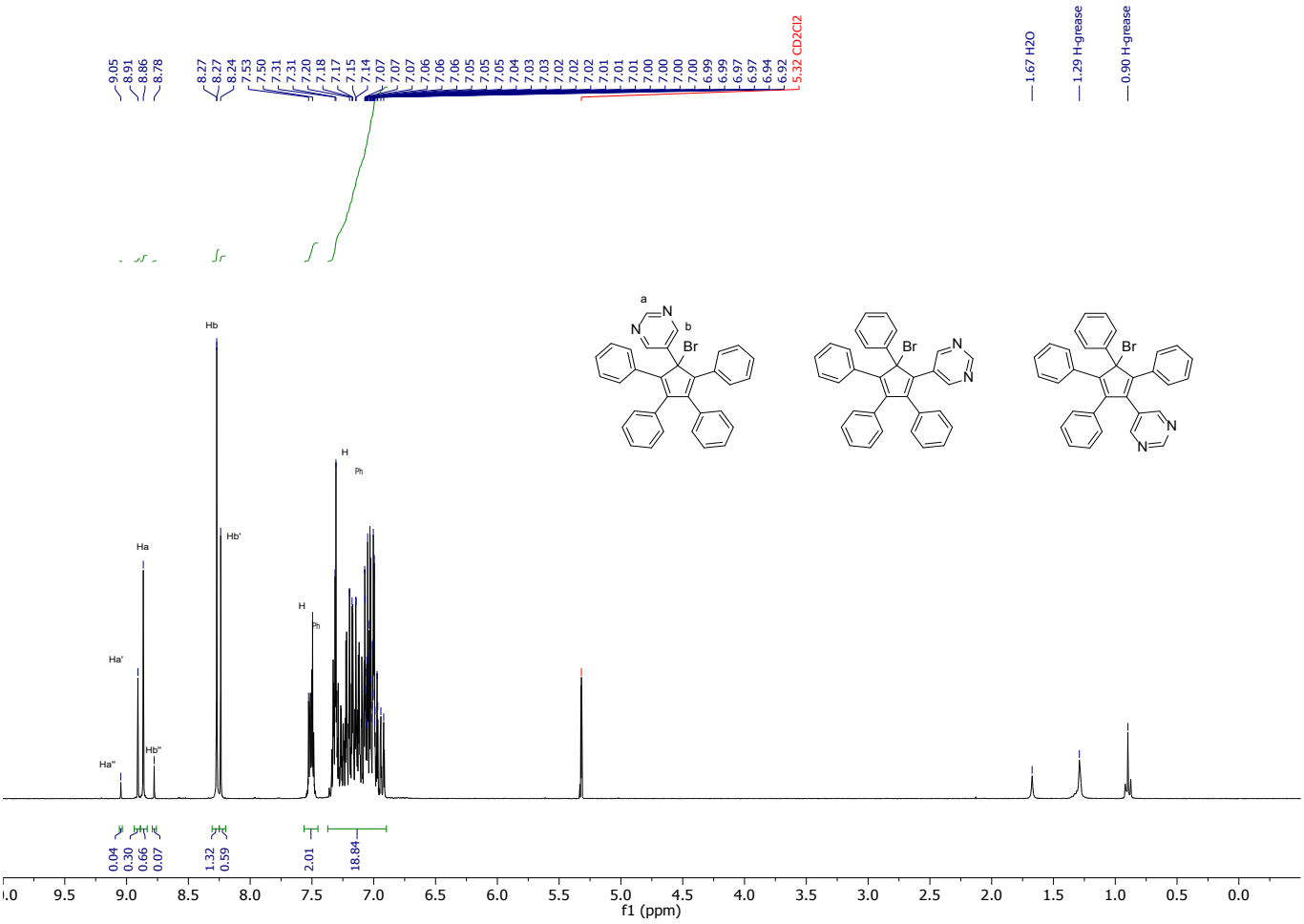

Figure S1: ^{1}H NMR Spectrum (300 MHz, CD_2Cl_2, 25 °C) of compound **3**, as a 66:30:4 mixture of three regioisomers

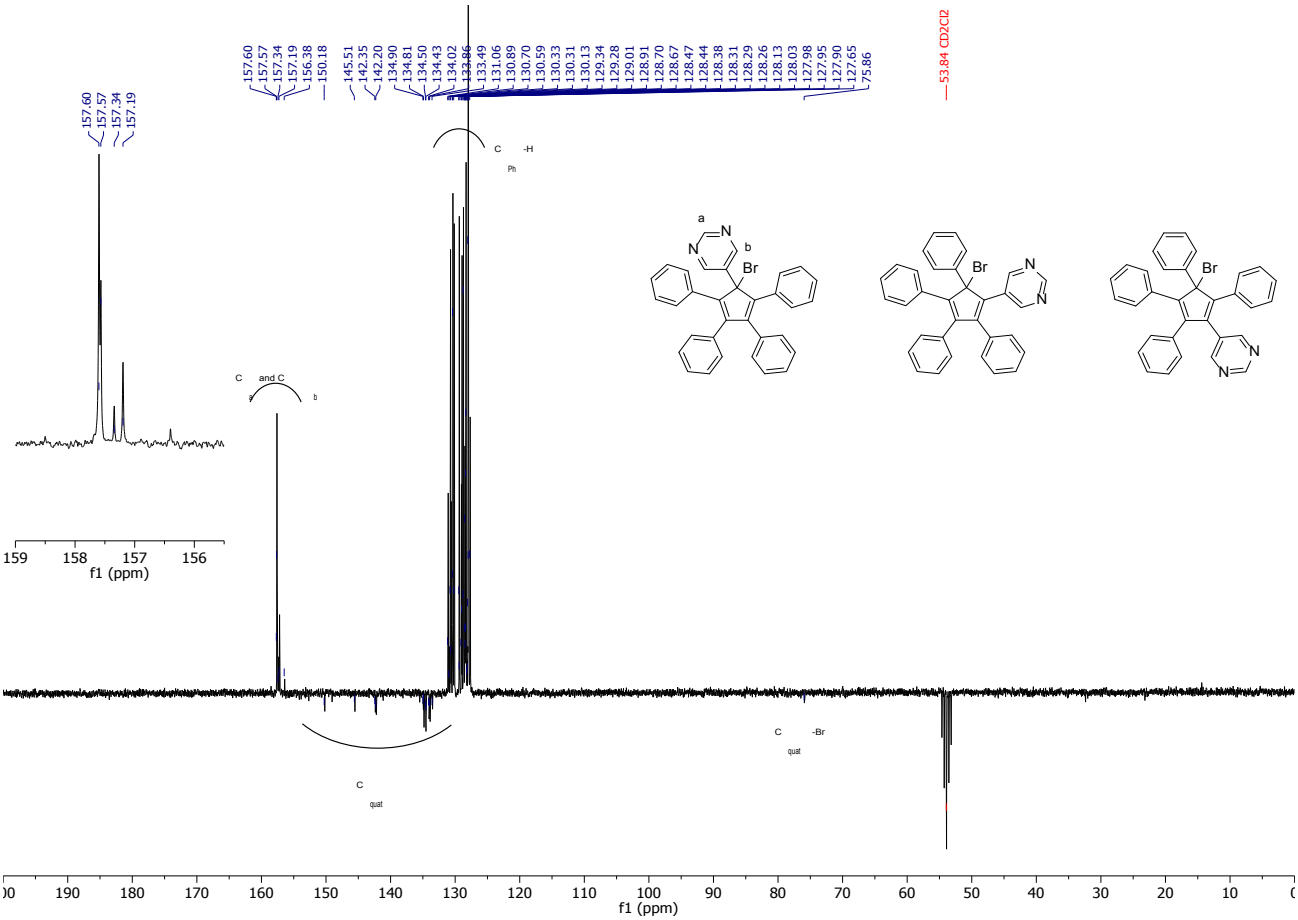

Figure S2: ^{13}C-Jmod NMR Spectrum (75 MHz, CD_2Cl_2, 25 °C) of compound **3**, as a 66:30:4 mixture of three regioisomers

2 Overview STM images of molecular gears on Au(111)

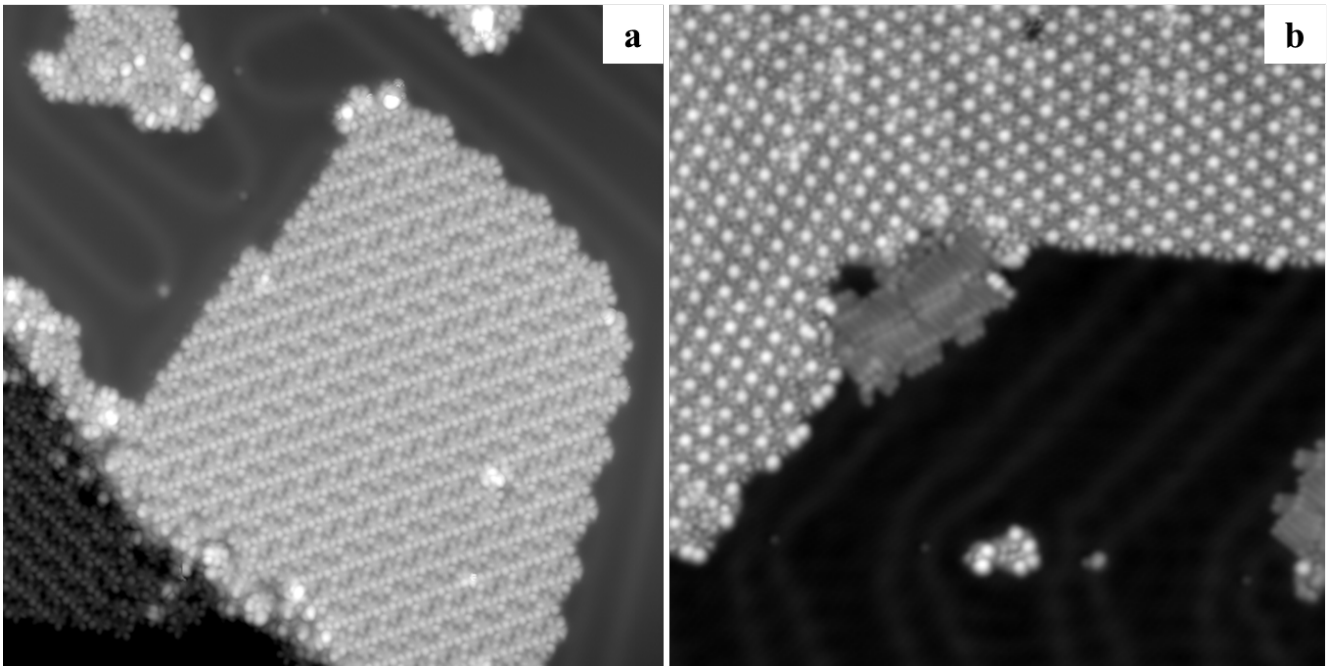

Figure S3: STM images of monolayers and islands formed by the molecular gears on Au(111). (a) Structure of the monolayers for gear **1**. (b) Structure of the monolayers for gear **2**. All STM images (40 nm x 40 nm) were taken under the conditions of V = 500 mV and I = 7.2 pA.

3 Density functional theory calculations of different adsorption sites

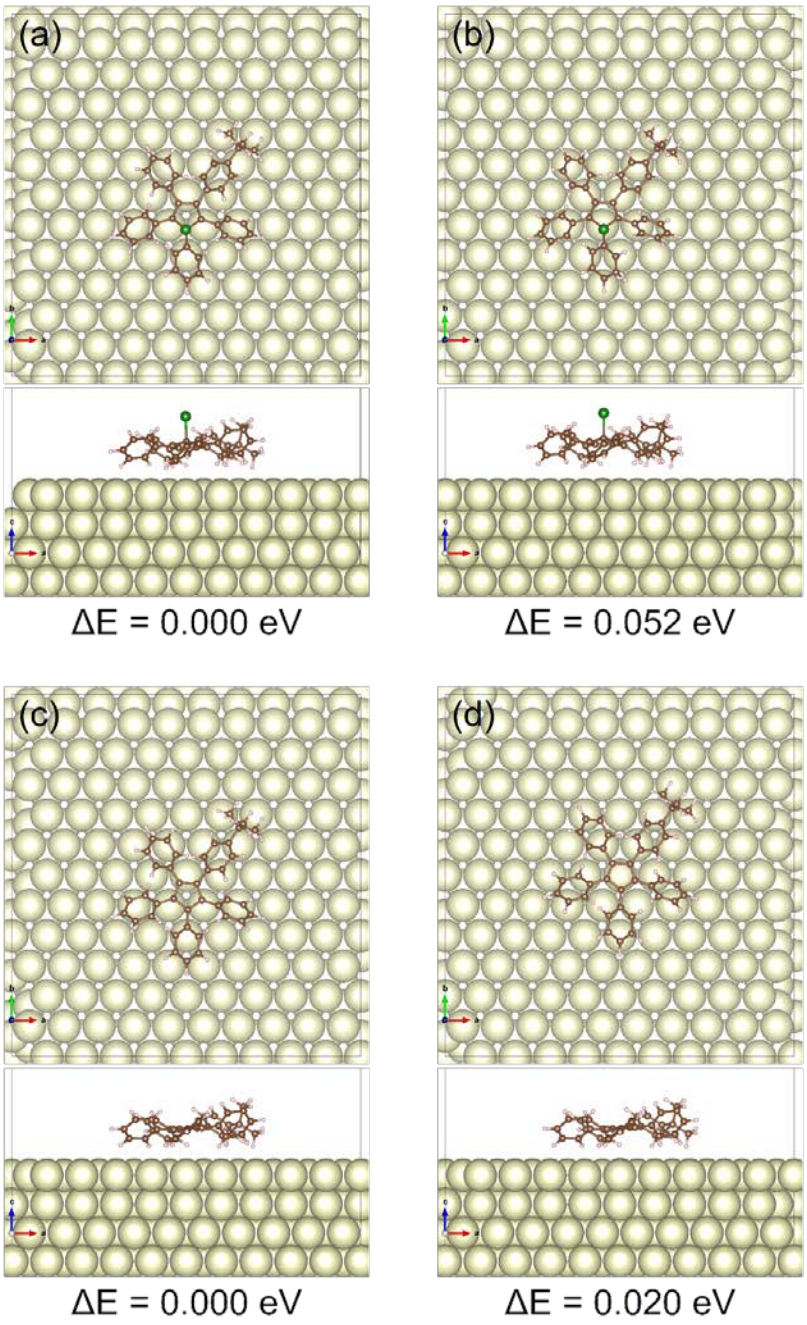

Figure S4: Different adsorption sites for the molecule with (a,b) and without Br (c,d). The energy difference between the configurations is small, revealing a quite flat energy surface.

4 Height profiles of molecular gears

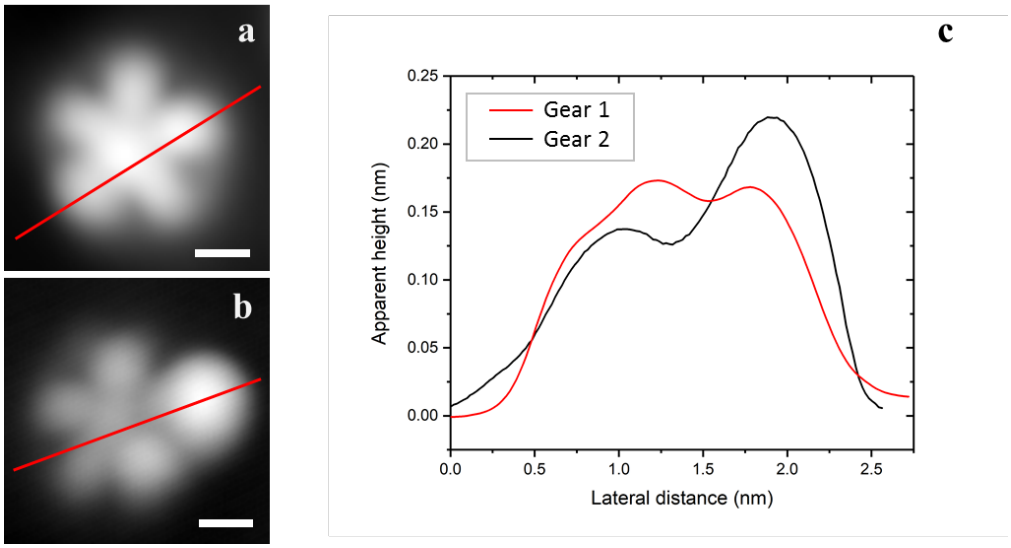

Figure S5: STM images of single molecular gears **1** and **2** on Au(111). (a – b) Red lines indicate the lateral profiles over the two molecules. (c) The graph shows the apparent height (nm) over the profiles on the molecules. Scale bar = 0.5 nm. All STM images were taken under the conditions of V = 500 mV and I = 7.2 pA.

5 Height profile determination of successful tip-induced debromination

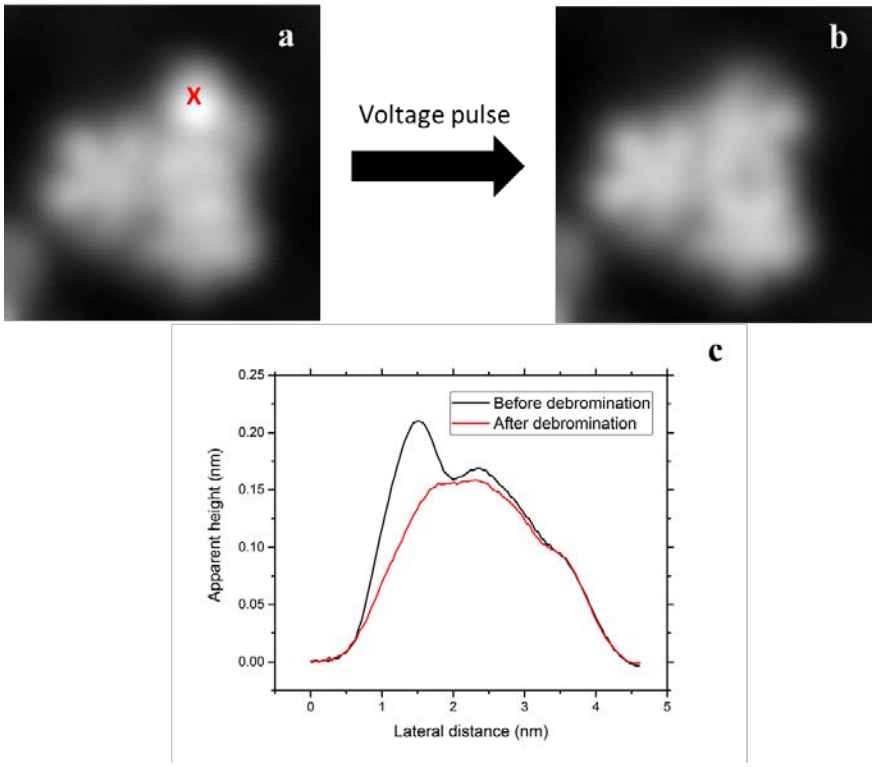

Figure S6: Tip-induced denromination on a gear **1** molecule. (a) A 3.0 V voltage pulse was locally applied. Position is marked as red cross. (b) The lobe with higher apparent height is flatten, indicating a successful debromination. All STM images (4.5 nm x 4.5 nm) are taken under V = 500 mV and I = 3.0 pA. (c) The graph shows the change of height profile before and after debromination over the profiles on the molecules.

6 Handle-like behavior between molecular gears 1

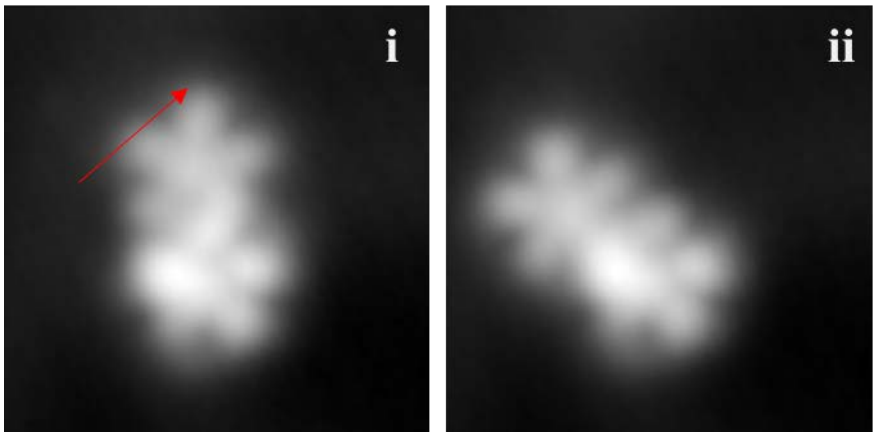

Figure S7: Handle-like behavior between molecular gears 1. (i – ii) Lateral manipulation (V = 30 mV and I = 8 pA; Tunneling resistance = 3.75 GΩ) on the driver gear generates a handle-like behavior of rotation in an opposite direction (red arrow for trajectory). All STM images (5 nm x 5nm) were taken under the conditions of V = 500 mV and I = 3 pA.

7 Failure of transmission of rotation due to interlocked *tert*-butyl teeth

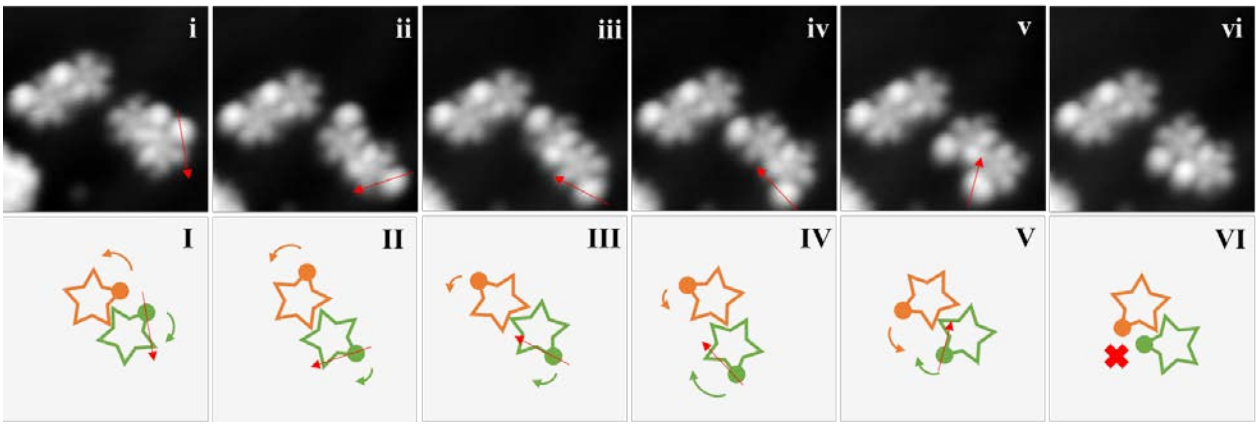

Figure S8: Stepwise collective rotation sequence between two single molecular gears 2. Red arrows indicate the trajectories of lateral manipulations (V = 10 mV and I = 14 pA; Tunneling resistance = 0.71 GΩ)achieved by STM tip. (i – vi) The rotations between two PPCP-tert-butyl molecular gears. (v - vi) The two *tert*-butyl teeth could not pass each other. No further rotation towards this direction. (I – VI) Corresponding schematic diagrams of the gear rotations (not in scale). All STM images (6.5 nm x 6.5nm) were taken under the conditions of V = 530 mV and I = 13 pA.

8 Detailed measured angle of rotation of molecular gears 2

a

Step	i – ii	ii – iii	iii – iv	iv – v	v - vi
Rotation angle	81.2°	90.9°	77.6°	63.8°	105.5°

b

Step	i – ii	ii – iii	iii – iv	iv – v	v - vi	vi - vii
Rotational angle for *driver*	57.2°	121.5°	116.2°	61.5°	64.2°	77.9°
Rotational angle for *follower*	48.7°	123.9°	90.3°	51.6°	4.5°	91.5°

c

Step	i – ii
Rotational angle for *driver*	63.9°
Rotational angle for *follower 1*	78.0°
Rotational angle for *follower 2*	103.8°

Table S1: Detailed measured angle of rotation of molecular gear 2. (a) Corresponding to the single molecule rotation sequence in Figure 5. (b) Corresponding to the two molecules collective rotation sequence in Figure 6. (c) Corresponding to the three molecules collective rotation sequence in Figure 7.

References

1. Vives, G. and G. Rapenne, *Directed synthesis of symmetric and dissymmetric molecular motors built around a ruthenium cyclopentadienyl tris(indazolyl)borate complex.* Tetrahedron, 2008. **64**(50): p. 11462-11468.
2. Schumann, H., C. Janiak, and J.J. Zuckerman, *Tetraphenylcyclopentadien und (4-tert-Butylphenyl)tetraphenylcyclopentadien: Synthese und Charakterisierung ihrer Alkalimetallsalze und Metallocene von Germanium, Zinn und Blei.* Chemische Berichte, 1988. **121**(2): p. 207-218.